Thermal unfolding and refolding of protein under osmotic pressure clarified by wide-angle X-ray scattering

ARTICLE *in* THERMOCHIMICA ACTA · MARCH 2012

Impact Factor: 2.18 · DOI: 10.1016/j.tca.2011.11.019

8 AUTHORS, INCLUDING:

Mitsuhiro Hirai
Gunma University
98 PUBLICATIONS **1,182** CITATIONS

SEE PROFILE

Rika Hirai
Gunma University
23 PUBLICATIONS **408** CITATIONS

SEE PROFILE

Thermochimica Acta 532 (2012) 15–21

Contents lists available at SciVerse ScienceDirect

Thermochimica Acta

journal homepage: www.elsevier.com/locate/tca

Thermal unfolding and refolding of protein under osmotic pressure clarified by wide-angle X-ray scattering

Mitsuhiro Hirai[a,*], Yoshiyuki Hagiwara[a], Kazuki Takeuchi[a], Ryota Kimura[a], Teruaki Onai[a], Rika Kawai-Hirai[b], Noboru Tohta[c], Masaaki Sugiyama[d]

[a] Department of Physics, Gunma University, Maebashi 371-8510, Japan
[b] Institute for Molecular and Cellular Regulation, Gunma University, Maebashi 371-8511, Japan
[c] Japan Synchrotron Radiation Research Institute, Sayo 679-5198, Japan
[d] Research Reactor Institute, Kyoto University, 590-0494, Japan

ARTICLE INFO

Article history:
Available online 1 December 2011

Keywords:
Protein folding
Osmotic pressure
Hydration
Wide-angle X-ray scattering

ABSTRACT

By using wide-angle X-ray scattering, we have studied the effect of osmotic pressure on protein unfolding and refolding of hen egg-white lysozyme (HEWL). The osmotic pressure was varied by adding polyvinylpyrrolidone (PVP). The increase of PVP concentration induced both the shortening of the intermolecular distance and the decrease of radius of gyration (R_g), indicating that PVP stabilizes HEWL to take another stable and compact structure. The decrement of R_g can be explained by a change of hydration-shell density accompanying a suppression of the intramolecular fluctuation by osmotic pressure. The increase of PVP concentration also stabilized the intermediate unfolded state, so-called a molten globule state in the thermal unfolding process at high osmotic pressure. The thermal reversibility of the structural transition was suppressed. The present results suggest that PVP works as a stabilizer for HEWL in the crowed solution through the changes both in the hydration shell and the intermolecular interaction.

1. Introduction

Hydration of biological macromolecules plays an important role in their structural stability and functions. Solvation of proteins is the key determinant for isothermal, concentration-dependent effects on protein equilibria, such as folding. The mechanism by which proteins fold into their native structures is one of the essential problems in biology [1–3]. As shown in the studies using such as inelastic neutron scattering and molecular-dynamics simulations, the dynamics of proteins is coupled with water molecules surrounding proteins [4–6]. So-called hydration shells of proteins are known to subject to the electrostatic properties of those local surface topologies. However, the role of hydration shells on protein folding is still under intensive issues in spite of many experimental and theoretical investigations. On the other hand, proteins are designed to function in environments crowded by co-solutes. Namely, the interior of a cell is very crowded with macromolecules, where the volume fraction of molecules reaches to be around 30–40% (v/v) [7]. Although there is no doubt that crowding changes protein equilibria, interpretations of the changes remain controversial since structural studies of protein folding and stability were conducted in dilute solutions in many cases. Based on experimental and thermodynamics theory, on the effect of small organic molecules, such as saccharides, polyolss, amino acids, and urea, on protein folding was shown to be explained well in terms of the solvation effects of those molecules as protecting and nonprotecting osmolytes on the denatured and native states of the protein [8,9]. However, how a protein folds into its native structure under a crowed condition created by high-macromolecular-weight co-solutes is still ambiguous.

We have carried out synchrotron radiation wide-angle X-ray scattering (SR-WAXS) experiments to clarify the effect of the change of osmotic pressure on the protein unfolding and refolding, where we have employed so-called “osmotic stress” method by adding a high molecular weight neutral polymer (osmolyte) into solutions. As one of the high molecular weight osmolytes, the use of polyvinylpyrrolidone (PVP) is well established [10,11] to study hydration forces as well as dextran [12]. PVP is also used as a nontoxic additive in various industrial products such as medicines, cosmetics, etc. On the other hand, we demonstrated previously that the SR-WAXS method using a third-generation synchrotron-radiation source enables us to observe the whole hierarchical structure of proteins from their quaternary or tertiary structures to secondary ones in solutions [13] and that the details of the unfolding–refolding process of proteins can be analyzed on all hierarchical structure levels and on structural transition cooperativity among them [14,15]. We have also found the

* Corresponding author at: Department of Physics, Gunma University, 4-2 Aramaki, Maebashi 371-8510, Japan. Tel.: +81 272 20 7554; fax: +81 272 20 7551.
E-mail address: mhirai@fs.aramaki.gunma-u.ac.jp (M. Hirai).

0040-6031/$ – see front matter © 2011 Elsevier B.V. All rights reserved.
doi:10.1016/j.tca.2011.11.019

collapse of the hydration shell of hen egg-white lysozyme (HEWL) prior to its thermal unfolding [16]. In other studies using small- and medium-angle X-ray scattering methods combined with the calorimetric measurements, we showed that the thermal unfolding transition of HEWL greatly depends on pH and on its structural hierarchy [17–19]. Based on the above previous results, the present study has been done to clarify an effect of osmotic pressure on native structure of HEWL in a crowed solution and on its thermal unfolding–refolding process by using WAXS method.

2. Experimental

2.1. Samples

HEWL of three times crystallized and polyvinylpyrrolidone (PVP, Mt. 40,000) were purchased from SIGMA Chemical Co. (USA). HEWL and PVP were used without further purification. All other chemicals used were of analytical grade. The buffer solvents used were 10 mM HEPES (*N*-(2-hydroxymethyl) piperazine-*N*′-(2-ethane-sulfonic acid)) buffer for pH 7 and 10 mM sodium acetate buffer for pH 3, 4, 5. HEWL solutions (5%, w/v) and PVP solutions with different concentrations (10, 20, 30, 40, 50%, w/w) were prepared for all buffer solvents. The above protein and PVP solutions were mixed by 1:1 in (v/v). Finally, we obtained the protein solutions (2.5%, w/v) at different PVP concentrations (5.2%, 10.5%, 16.2%, 21.9%, and 27.9% PVP (w/v) that correspond to the osmotic pressure of 1.40×10^4, 4.44×10^4, 1.17×10^5, 2.50×10^5, and 4.78×10^5 (N/m^2), respectively [10].). The densities of PVP solutions were measured by using the electronic balance 1712MP8 of Sartorius Co.

2.2. Wide-angle X-ray scattering and analyses

Wide-angle X-ray scattering (WAXS) measurements were performed by using the spectrometer installed at BL-40B2 beam port of the 8 GeV synchrotron radiation source (SPring-8) at the Japan Synchrotron Radiation Research Institute (JASRI), Harima, Japan. The X-ray scattering intensity was recorded by the R-AXIS IV from RIGAKU Co. The X-ray wavelengths and the sample-to-detector distances were 1.0 Å and 51 cm, respectively. Sample cells composed of a pair of thin-quartz windows with 1 mm path length were used. Meanwhile the measurements, the sample solutions were slowly oscillated. Under the present measurement conditions, some radiation damages were negligible due to the small beam size (~0.1 mm^2) as reported previously [13,14]. The exposure time for each measurement was 30 s. In the WAXS measurements, the temperature of the sample-cell holder was controlled at an appropriate temperature by using a water-bath circulator. The background correction of WAXS data was described in detail in elsewhere [13,14]. The radius of gyration R_g was determined by using the following equation.

$$R_g^2 = \frac{\int_0^{D_{max}} p(r) r^2 \, dr}{2 \int_0^{D_{max}} p(r) \, dr} \quad (1)$$

where the $p(r)$ is the distance distribution function calculated by the Fourier inversion of the observed scattering intensity $I(q)$ ($q = (4\pi/\lambda)\sin(\theta/2)$; θ and λ are the scattering angle and the X-ray wavelength), and D_{max} is the maximum diameter of the solute particle determined by the $p(r)$ function satisfying the condition $p(r) = 0$ when $r > D_{max}$. The $p(r)$ function is defined as

$$p(r) = \frac{1}{2\pi^2} \int_0^{\infty} rqI(q) \, \sin(rq) \, dq \quad (2)$$

In the estimation of R_g, the use of Eq. (1) is known to reduce some inherent systematic errors caused by concentration or aggregation effects in comparison with the use of the Guinier approximation [20].

3. Results and discussion

3.1. How to clarify hierarchal structures of proteins in solution by wide-angle X-ray scattering

In a series of our studies on protein folding [13–19], we show that small-angle X-ray scattering (SAXS) and WAXS data with high statistic precision enable us to analyze not only a change of a whole structure (quaternary and/or tertiary structure) of a protein but also its internal structures such as domain and secondary structures as shown previously [13,14]. Fig. 1 takes up the scattering curve of HEWL as an example showing schematically the correspondence between different hierarchal structure levels and scattering curves, where both of the experimental data of HEWL (5%, w/v, at pH 5 at 25 °C) and the theoretical scattering curve obtained by using the CRYSOL program are shown. The CRYSOL program is known to calculate a scattering curve of a protein in solution from the atomic coordinates of the protein by taking into account of a hydration shell surrounding the protein [21]. As shown in Fig. 1, the scattering curve of a protein in different q-regions (A–D regions in Fig. 1) mostly correspond to different hierarchical structure levels, that is, the quaternary and/or tertiary structure ($q < \sim 0.2$ Å^{-1}), the inter-domain correlation (~ 0.25 Å$^{-1} < q < \sim 0.5$ Å^{-1}) and intra-domain

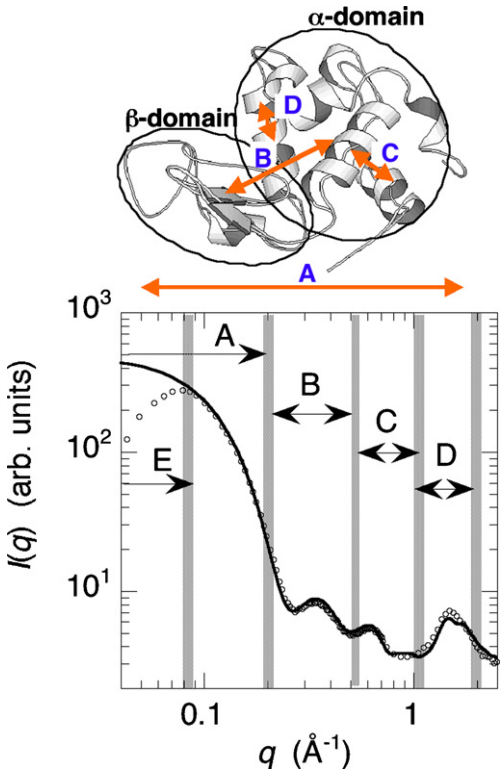

Fig. 1. Relation between WAXS curve and typical intramolecular distances within the HEWL molecule shown schematically with its three-dimensional structure. Both theoretical (—) and experimental (o) WAXS curves of HEWL (5%, w/v at pH 4.5, 24 °C) are shown. The theoretical WAXS curve was obtained by using CRYSOL program [19]. The scattering curves in the regions of parts A ($q < \sim 0.2$ Å^{-1}), B (~ 0.25 Å$^{-1} < q < \sim 0.5$ Å^{-1}), C (~ 0.5 Å$^{-1} < q < \sim 0.8$ Å^{-1}), and D (~ 1.1 Å$^{-1} < q < \sim 1.9$ Å^{-1}) correspond to different hierarchical structure levels, that is, the tertiary structure, the inter-domain correlation and intra-domain structure, and the secondary structures including the closely packed side chains, respectively. The broad peak in the region E ($q < \sim 0.1$ Å^{-1}) reflects the presence of repulsive interparticle interaction between the proteins. The schematic picture and the WAXS curve are reproduced from the previous report [12].

structure ($\sim$0.5 Å^{-1} < q < $\sim$0.8 Å^{-1}), and the secondary structures, including the closely packed side chains ($\sim$1.1 Å^{-1} q < $\sim$1.9 Å^{-1}), respectively. In addition, for the case of HEWL solution at low ionic strength and at less than pH 7, an inter-particle correlation peak appears in a small-q region (q < $\sim$0.07 Å^{-1}, E region in Fig. 1) due to an electrostatic repulsion between the proteins. Although the correlation peak shifts to higher q with increasing the protein concentration, the presence of the repulsive interaction is important to suppress some aggregation in unfolding–refolding processes of HEWL, which does not affect the scattering curve above q = $\sim$0.1 Å^{-1} under the present condition as same as in the previous studies [14,16–19]. Alternatively, for small proteins such as HEWL, the scattering curve below $\sim$0.1 Å^{-1} gives us another information on an inter-particle interaction potential between proteins that would ordinary depend on an effective surface charge of the protein as a polyelectrolyte. In a special case that the structure of a solute particle can be regarded to be uniform and to have a simple geometry such as a sphere, we can actually estimate an effective charge of a solute particle [22]. The above general understanding of WAXS curves of systems with some structural hierarchy is quite important and useful, especially for studies of proteins in solutions. Further details of WAXS data treatments based on theoretical considerations of protein hierarchical structures have been shown in elsewhere [23,24].

3.2. Effect of osmotic pressure on HEWL structure at different pH

Fig. 2 shows the PVP concentration dependence of the WAXS curve of HEWL (2.5%, w/v) at different pH values at 25 °C. The PVP concentration was varied from 0 to 27.9% (w/v), which corresponds to the rise of osmotic pressure from 0 to 4.78 × 10^5 (N/m^2), namely from 0 to 4.11 atmospheric pressure. The broad peak below q = $\sim$0.07 Å^{-1} results from an electrostatic repulsion between the proteins. By the addition of PVP, the position of the peak shifts gradually from $\sim$0.06 Å^{-1} to $\sim$0.065 Å^{-1}, indicating the shortening of the inter-molecular distance between the proteins from $\sim$105 Å to $\sim$97 Å. This change of the inter-molecule distance ($\sim$8% decrease) agrees well with the $\sim$9% decrease expected from the excluded volume effect by PVP. In the scattering curve in the range of $\sim$0.1–0.2 Å^{-1}, corresponding to the tertiary structure, the slope becomes smaller with increasing the PVP concentration from 0 to 27.9% (w/v) for every pH, which is attributable to the contraction of the whole structure (shape and dimension) of HEWL including its hydration shell. This contraction is also suggested by the other analyses as shown below. According to the theoretical simulation of wide-angle scattering profiles of various types of proteins [13,23,24], it should be mentioned that the profiles of proteins below $\sim$0.2 Å^{-1} is governed by large-scaled structures such as quaternary and tertiary structures, alternatively, molecular shape and dimension, and intermolecular interaction. In addition, the intensities below $\sim$0.2 Å^{-1} also depend on the difference between the average scattering densities, so-called contrast $\Delta\rho$, of the solute particle and the solvent. The modulated profiles below $\sim$0.25 Å^{-1} mostly depend on local structures such as intramolecule structures, alternatively, on some heterogeneity within molecules. Some variations in contrast contribute to shift of background scattering intensities, but not to change the characteristic of the modulations. The above understandings are based on the theoretical basis that the scattering function of a protein consists of the three basic scattering functions, namely, that of the shape, the scattering-density-fluctuation function within the protein, and the interference term between them where the second term

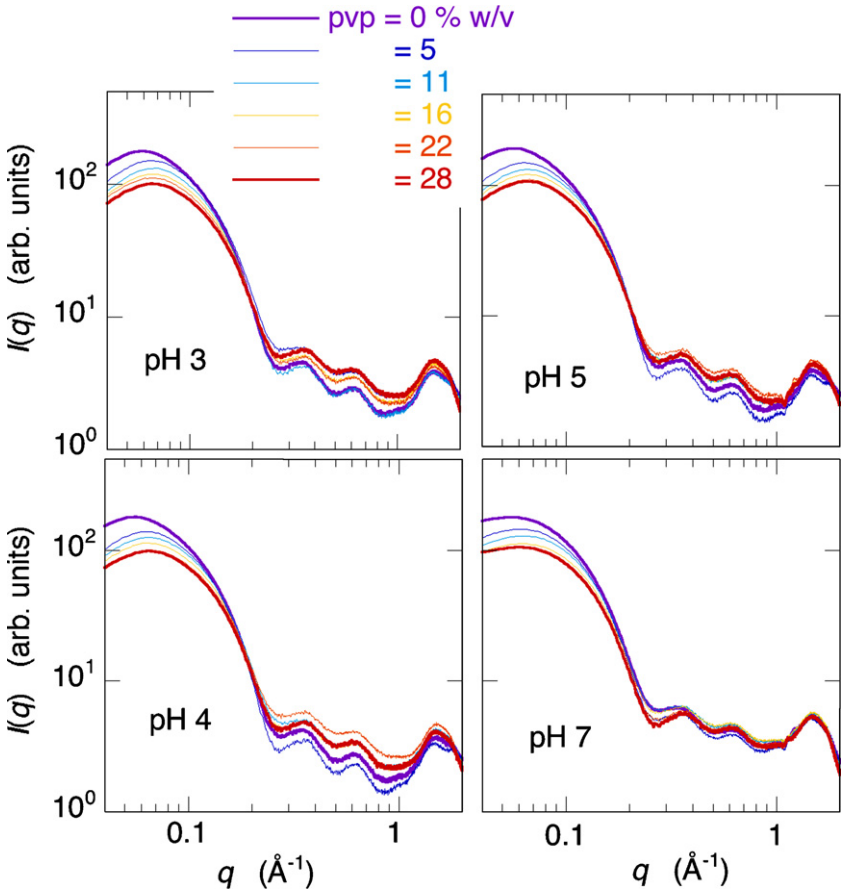

Fig. 2. PVP concentration dependence of WAXS curve of lysozyme (2.5%, w/v) at 25 °C at different pH, where the PVP concentration was varied from 0 to 28% (w/v).

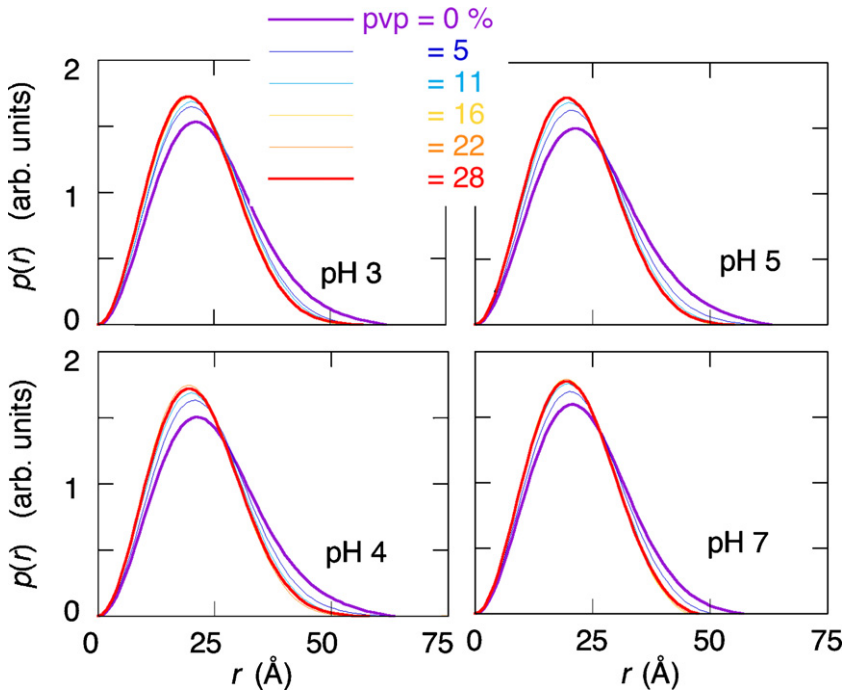

Fig. 3. Distance distribution function $p(r)$ of lysozyme (2.5%, w/v, at 25 °C) depending on PVP concentration, which was obtained from WAXS curves in Fig. 2.

(intermolecular scattering function) does not depend on contrast [25]. On the other hand, from the scattering curve above ~0.25 Å^{-1} we can recognize some difference of the effect of PVP on the intramolecular structure. At pH 7 the changes in the domain and secondary structures seem to be smaller than those at other pH. On the contrary, at low pH such an influence tends to appear more clearly. However, the above change is relatively small and the scattering curve above ~0.25 Å^{-1} mostly holds the characteristic profile of HEWL at the initial state. Thus, the PVP addition affects the intramolecular structure of HEWL a little to keep its native state.

Fig. 3 shows the distance distribution function $p(r)$ obtained from the WAXS curves in Fig. 1 by using Eq. (2). The $p(r)$ function is well known to depend on shape and internal scattering density distribution of a particle [18]. At every pH, the r-values of the peak position and the intercept against the abscissa (maximum dimension D_{max} of a solute particle) gradually decrease with increasing the PVP concentration, indicating clearly the contraction or shrinkage of the protein structure by osmotic pressure. Fig. 4 summarizes the PVP dependence of radius of gyration R_g at different pH. The R_g value shows a simple decreasing-tendency for every pH. The decrement of R_g becomes to be smaller above PVP = ~16% (w/v). The R_g value changes from ~16 Å to ~14 Å at pH 3, 4, and 5, and from ~15 Å to ~13 Å at pH 7. This level of reduction in R_g is mainly attributable to the change of the hydration shell density, namely, a collapse of hydration shell, as shown below. The study of proteins using X-ray and neutron solution scattering techniques indicate the existence of a hydration shell whose average density is around 10% larger than that of the bulk water [26], which was supported by the subsequent molecular dynamics simulations [5,6]. As shown previously [16] based on the crystal structure using the CRYSOL program [21], the change of the HEWL hydration shell density from 1.1 to 1.0 reduces the R_g value in ~10% (from 15.64 Å to 14.06 Å in R_g). On the other hand, the R_g value of a solute particle in a solution is known to depend on the contrast $\Delta\rho$ as followed [25].

$$R_g^2 = R_{g0}^2 + \frac{\alpha}{\Delta\rho} - \frac{\beta}{(\Delta\rho)^2}$$

where R_{g0}, mechanical radius of gyration; α and β are the factors depending on internal scattering density fluctuation and on the difference between the geometrical center and the scattering density center of the particle. According to the atomic coordinates of HEWL, both α and β factors are obtained to be 36.2 Å^2/cm^2 and −3.5 Å^2/cm^4. By adding PVP from 0% (w/v) to 27.9% (w/v), the electron density of the solvent becomes higher due to the increase of the density from 1.0085 g/ml to 1.0655 g/ml. Then, the contrast of HEWL changes from 0.0846 e/Å^3 to 0.0677 e/Å^3, namely from 2.36×10^{10} cm^{-2} to 1.90×10^{10} cm^{-2}. This change of contrast increases the R_g value in ~0.9%. Therefore, the collapse of the hydration shell would accompany a compaction of the HEWL tertiary structure due to a suppression of the fluctuation within the molecule induced by osmotic pressure. However, the above results suggest that the addition of PVP destroys the hydration shell of HEWL mostly without affecting the intramolecular structure.

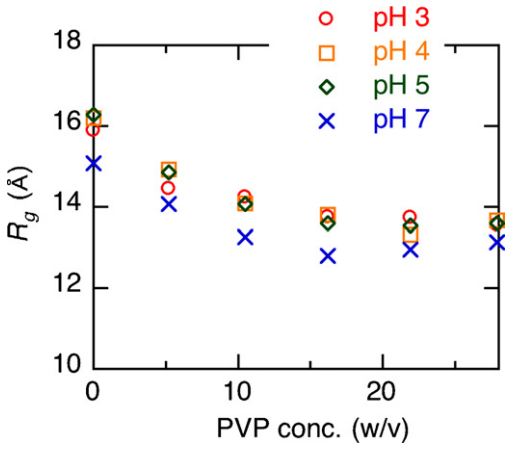

Fig. 4. Radius of gyration R_g of lysozyme (2.5%, w/v, at 25 °C) depending on PVP concentration at different pH.

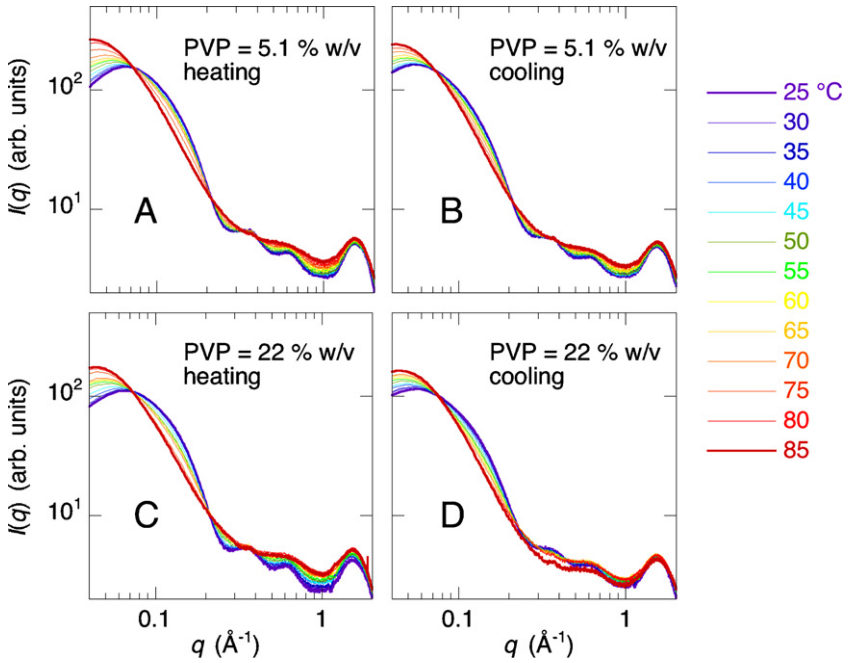

Fig. 5. Reversibility of WAXS curves in thermal unfolding–refolding processes of lysozyme under osmotic pressure at pH 3, where A, unfolding at PVP = 5.1% (w/v); B, refolding at PVP = 5.1% (w/v); C, unfolding at PVP = 21.9% (w/v); D, refolding at PVP = 21.9% (w/v).

3.3. *Thermal unfolding and refolding of HEWL under osmotic pressure at different pH*

In the previous reports [14–19], by using X-ray scattering and differential scanning calorimetry we clarified the detailed characteristics of thermal structural transition of HEWL depending on pH. We succeed to observe the unfolding and refolding processes of HEWL at low pH values by using WAXS and to show high reversibility [14,19] from the tertiary structure to the secondary one. The conditions of HEWL solutions in the above studies were as same as in the present experiment. Based on the previous results, we have studied the thermal reversibility of HEWL depending on pH. Fig. 5 shows the thermal unfolding and refolding processes of HEWL at pH 3 under the presence of PVP = 5.2% (w/v) and 21.9% (w/v). In comparison with the case at PVP = 5.2% (w/v) in Fig. 5A and B, the WAXS curve at PVP = 21.9% (w/v) in Fig. 5A and B becomes to be less reversible in the whole q region. Especially, the modulated profile in the WAXS curve ranging from ~0.25 $Å^{-1}$ to ~0.8 $Å^{-1}$, corresponding to both of the inter-domain correlation and the intra-domain structure, does not recover to the initial state, meaning the irreversibility of the intra-molecular structure is enhanced with the elevation of osmotic pressure. Thus, the addition of the PVP evidently obstructs

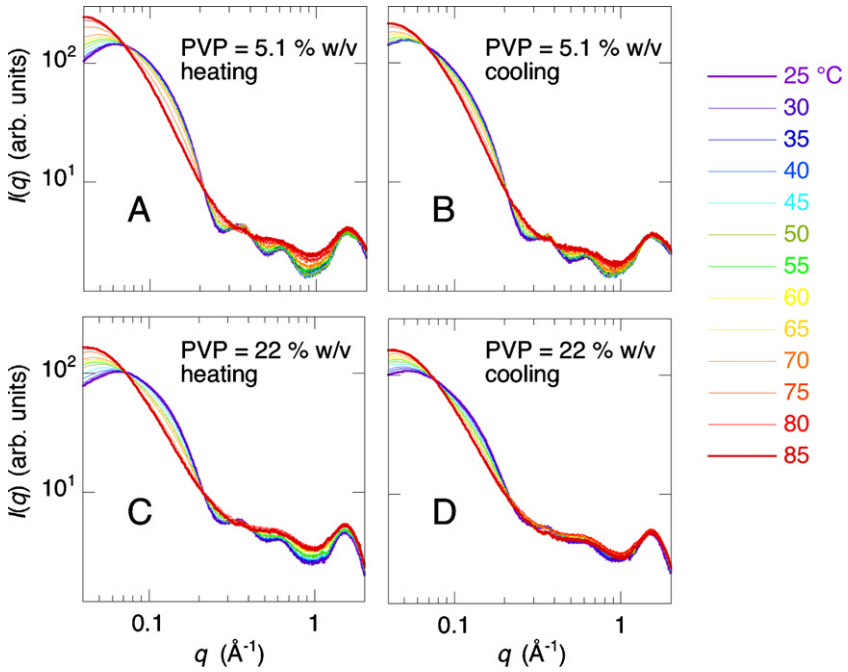

Fig. 6. Reversibility of WAXS curves in thermal unfolding–refolding processes of lysozyme under osmotic pressure at pH 4, where A–D are as in Fig. 5.

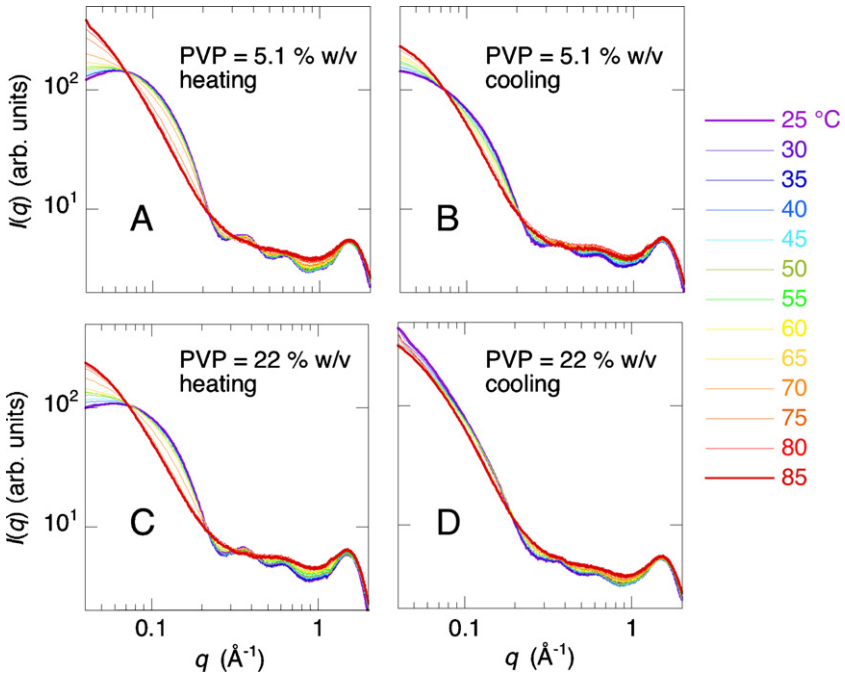

Fig. 7. Reversibility of WAXS curves in thermal unfolding–refolding processes of lysozyme under osmotic pressure at pH 7, where A–D are as in Fig. 5.

the refolding of lysozyme that should be intrinsically reversible in the whole hierarchal structure levels. As shown in Fig. 6, the irreversibility in the thermal unfolding–refolding process at pH 4 caused by osmotic pressure becomes to be more remarkable, especially at PVP = 21.9% (w/v). The characteristics of the thermal unfolding and refolding at pH 5 resemble those at pH 4 (data omitted).

On the other hand, in comparison with the cases at pH 3, 4 and 5, the irreversibility of the structural transition is much clearly seen at pH 7, as shown in Fig. 7. Particularly at PVP = 21.9% (w/v), the structural transition is mostly irreversible. We can recognize an evident difference between the thermal unfolding processes at pH 7 and below pH 5. At pH 7 the scattering intensity below $q = \sim 0.06\,\text{Å}^{-1}$ significantly increased with the rise of temperature, which accompanied by the disappearance of the broad peak at $\sim 0.06\,\text{Å}^{-1}$ that reflects the repulsive inter-molecular interaction. As the isoelectric point of HEWL is known to be ~11, the repulsive electrostatic force between the proteins at pH 7 should be weaker than in the cases below pH 5. Therefore, the above change of the WAXS curve below $q = \sim 0.06\,\text{Å}^{-1}$ indicates the appearance of the aggregates of the denatured proteins at high temperature. Both of the weaker inter-molecular interaction and the shortening of the inter-molecular distance by osmotic pressure would attribute to the irreversibility of the structural transition especially for PVP = 21.9% (w/v) at pH 7.

Fig. 8 summarizes the temperature dependence of radius of gyration R_g of HEWL in the thermal unfolding–refolding processes

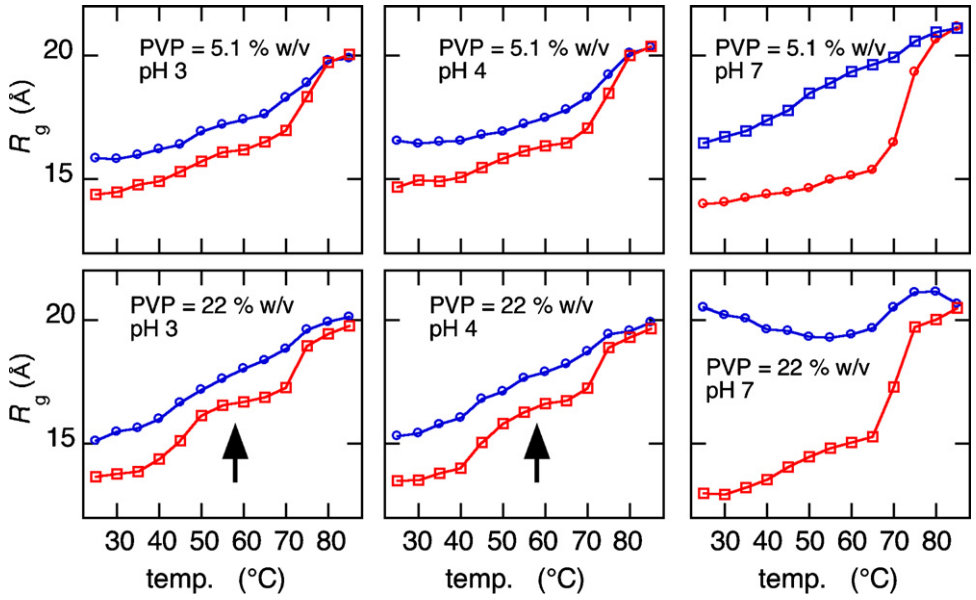

Fig. 8. Comparison of reversibility of radii of gyration of lysozyme in thermal unfolding–refolding processes under osmotic pressure at different pH, where A and B, at pH 3, PVP = 5.1% (w/v), 22% (w/v); C and D, at pH 4, at PVP = 5.1% (w/v), 22% (w/v); E and F, at pH 7, at PVP = 5.1% (w/v), 22% (w/v). The marks of red square and blue circle correspond to the heating (unfolding) process and the cooling (refolding) one, respectively. The arrows indicate intermediate states. (For interpretation of the references to color in this figure legend, the reader is referred to the web version of this article.)

under osmotic pressure at different pH. Although the exact definition of the transition temperature of R_g is a little difficult in Fig. 8 due to a relatively gradual change of R_g, the main transition temperature at low pH clearly shifts to a higher temperature in comparison with the case of thermal unfolding of HEWL without osmotic pressure [17–19]. A thermal hysteresis in the unfolding–refolding process under the presence of PVP is seen at every pH. The hysteresis, namely, the irreversibility is more evident both at high pH and at PVP = 21.9% (w/v). Noticeably, in the unfolding process under osmotic pressure the R_g value tends to show a two-step transition, which appears much evidently at low pH (at pH 3 and 4, also at pH 5, data not shown) under high osmotic pressure (at PVP = 21.9%, w/v, Fig. 8) as a plateau region of R_g in the range of ~40–50 °C. It suggests that an intermediate state with a partially unfolded structure, so-called a molten globule state is stabilized under osmotic pressure.

4. Conclusion

We have quantified the effect of osmotic pressure on the structure of HEWL and its thermal unfolding–refolding processes by using the osmotic stress method and PVP as an osmolyte. The reduction of R_g and the change of $p(r)$ function induced by the elevation of osmotic pressure clearly indicate that PVP works as a stabilizer for HEWL to take another stable and compact structure. The decrement of R_g (~12–13%) observed is mostly comparable with the theoretically estimated value (~10%) at least when assuming that the hydration shell surrounding the protein surface is collapsed. The rest of the decrement would be attributable to the suppression of the intramolecular fluctuation by osmotic pressure. The osmotic pressure is known to be an entropic force given by $\Delta S(dT_m/d\Pi_m) = v_w \Delta N_w$ (where ΔS, the change in entropy/residue; T_m, the transition temperature; Π_m, transition osmotic pressure; ΔN_w, the change in the number of preferentially included water molecules/residue; v_w, the molecular volume of water) [27]. According to the above relation, ΔS should be negative since ΔN_w is negative and $(dT_m/d\Pi_m)$ is positive. Thus, it would be possible that the load of osmotic pressure changes the energetic function of protein, so-called energetic landscape, through the change of hydrated water [28,29]. Under the new stable state of HEWL induced by osmotic pressure, the intermediate state in the thermal unfolding transition also tends to be stabilized due to the influence of osmotic pressure on the landscape of HEWL. Based on the thermodynamic considerations of the solvation effects of osmolytes [8], the derivative of the free energy difference between the native and the denatured states under the presence of PVP should be expected to be positive in sign, which might explain the appearance of more compact structure at the native state and at the transition intermediate.

Acknowledgments

The work was performed under the approvals of the Photon Factory Program Advisory Committee of KEK (Proposal No. 2008G095) and of the JASRI program advisory committee (Proposal No. 2007B1033 & 2008A1035 & 2011B1923).

References

[1] R.H. Pain (Ed.), Mechanisms of Protein Folding, Oxford University Press, 2000.
[2] C.M. Dobson, Nature 426 (2003) 884–890.
[3] M. Oliveberg, P.G. Wolynes, Q. Rev. Biophys. 38 (2005) 245–288.
[4] F. Gabel, D. Bicout, U. Lehnert, M. Tehei, M. Weik, G. Zaccai, Q. Rev. Biophys. 35 (2002) 327–367.
[5] V.A. Makarov, B.K. Andrews, P.E. Smith, B.M. Pettitt, Biophys. J. 79 (2000) 2966–2974.
[6] S.G. Dastidar, C. Mukhopadhyay, Phys. Rev. E 68 (2003) 21921–21930.
[7] D.S. Goodsell, Trends Biochem. Sci. 16 (1991) 203–206.
[8] J. Rösgen, B.M. Pettitt, D.W. Bolen, Biophys. J. 89 (2005) 2988–2997.
[9] J. Rösgen, B.M. Pettitt, D.W. Bolen, Biochemistry 43 (2004) 14472–14484.
[10] T.J. McIntosh, S.A. Simon, Biochemistry 25 (1986) 4058–4066.
[11] S.T. Nagle, H.I. Petrache, J.F. Nagle, Biophys. J. 75 (1998) 917–925.
[12] D.M. Leneveu, R.P. Rand, V.A. Parsegian, Biophys. J. 18 (1977) 209–230.
[13] M. Hirai, H. Iwase, T. Hayakawa, K. Miura, K. Inoue, J. Synchrotron Radiat. 9 (2002) 202–205.
[14] M. Hirai, M. Koizumi, T. Hayakawa, H. Takahashi, S. Abe, H. Hirai, K. Miura, K. Inoue, Biochemistry 43 (2004) 9036–9049.
[15] M. Koizumi, M. Hirai, K. Inoue, Bunseki Kagaku 55 (2006) 411–418.
[16] M. Koizumi, H. Hirai, T. Onai, K. Inoue, M. Hirai, J. Appl. Crystallogr. 40 (2007) s175–s178.
[17] M. Hirai, S. Arai, H. Iwase, T. Takizawa, J. Phys. Chem. B 102 (1998) 1308–1313.
[18] M. Hirai, S. Arai, H. Iwase, J. Phys. Chem. B 103 (1999) 549–556.
[19] S. Arai, M. Hirai, Biophys. J. 76 (1999) 2192–2197.
[20] L.A. Feigin, D.I. Svergun, Structure Analysis by Small Angle X-ray and Neutron Scattering, Plenum Press, New York, 1987.
[21] D.I. Svergun, C. Barberato, M.H.J. Koch, J. Appl. Crystallogr. 28 (1995) 768–773.
[22] M. Hirai, T. Takizawa, S. Yabuki, K. Hayashi, J. Phys. Chem. B 103 (1999) 10136–10142.
[23] M. Hirai, Synchrotron Radiat. 19 (2006) 437–443 (in Japanese).
[24] M. Hirai, in: T. Imae, T. kanaya, M. Furusaka, N. Torikai (Eds.), Neutrons in Soft Matter, A John Wiley & Sons, 2011, pp. 351–382.
[25] H.B. Stuhrmann, A. Miller, J. Appl. Crystallogr. 11 (1978) 325–345.
[26] D.I. Svergun, S. Richard, M.H.J. Koch, Z. Sayers, S. Kuprin, G. Zaccai, Proc. Natl. Acad. Sci. U.S.A. 95 (1998) 2267–2272.
[27] C.B. Stanley, H.H. Strey, Biophys. J. 94 (2008) 4427–4434.
[28] K.A. Dill, H.S. Chan, Nat. Struct. Biol. 4 (1997) 10–19.
[29] Y. Levy, J.N. Onuchic, Annu. Rev. Biophys. Biomol. Struct. 35 (2006) 389–415.